IOP Publishing Journal of Physics A: Mathematical and Theoretical
J. Phys. A: Math. Theor. **48** (2015) 125101 (12pp) doi:10.1088/1751-8113/48/12/125101

Co-existing hidden attractors in a radio-physical oscillator system

A P Kuznetsov[1], S P Kuznetsov[1], E Mosekilde[2] and N V Stankevich[3]

[1] Kotel'nikov's Institute of Radio-Engineering and Electronics of RAS, Saratov Branch, Zelenaya 38, Saratov, 410019, Russian Federation
[2] Department of Physics, The Technical University of Denmark, Fysikvej 309, DK-2800 Lyngby, Denmark
[3] Yuri Gagarin State Technical University of Saratov, Politehnicheskaya 77, Saratov, 410054, Russian Federation

E-mail: stankevichnv@mail.ru

Received 25 June 2014, revised 29 October 2014
Accepted for publication 10 November 2014
Published 2 March 2015

Abstract

The term 'hidden attractor' relates to a stable periodic, quasiperiodic or chaotic state whose basin of attraction does not overlap with the neighborhood of an unstable equilibrium point. Considering a three-dimensional oscillator system that does not allow for the existence of an equilibrium point, this paper describes the formation of several different coexisting sets of hidden attractors, including the simultaneous presence of a pair of coinciding quasiperiodic attractors and of two mutually symmetric chaotic attractors. We follow the dynamics of the system as a function of the basic oscillator frequency, describe the bifurcations through which hidden attractors of different type arise and disappear, and illustrate the form of the basins of attraction.

Keywords: hidden attractors, radio-physical oscillator, coexisting chaotic states, absence of an equilibrium state

(Some figures may appear in colour only in the online journal)

1. Introduction

Most autonomous, nonlinear dynamic systems that have been studied so far display a structure in which stable periodic, quasiperiodic or chaotic attractors coexist with one (or more) unstable equilibrium points. This is true for the celebrated Lorenz [1] and Rössler [2] oscillators and it is also true for a broad range of other systems that have served as paradigms for the development of nonlinear dynamics. A structure of this form is intuitively acceptable

as it conforms with the general understanding that nonlinear dynamic behaviors in autonomous systems develop through destabilization of an original equilibrium state as, with increasing excitation, a cascade of bifurcations leads the system through states of growing complexity. The essential point is here that, although destabilized, the original equilibrium point continues to exist. In this connection it is interesting to recall, for instance, how the presence of an unstable equilibrium point plays an essential role in Shil'nikov's famous criterion for the onset of chaos [3, 4].

To the extent that they have been known to exist, complex dynamic systems without an equilibrium point have mostly been considered as un-physical or mathematically incomplete. However, as experience shows, a system that exhibits complex nonlinear dynamic behavior does not need to also display an unstable equilibrium state [5–7]. During the last few years, a rapidly growing number of studies have been published in which quasiperiodic or chaotic attractors are shown to exist in the absence of any form of equilibrium point [8] or in the presence of only stable equilibrium points [9]. Wang *et al* [10] and Wei *et al* [11] have recently demonstrated the existence of a hyperchaotic attractor in a 4D system without equilibria, and Kuznetsov *et al* [12, 13] have described the development of quasiperiodicity in a model of a radio-physical oscillator that does not display an equilibrium point. Through a clever search of system space, Jafari *et al* [14] have established a list of 17 structurally different 3D systems that display quadratic chaotic flows without equilibria. Wang and Chen [15] have demonstrated how one can construct chaotic systems with any number of equilibria, and Chaudhuri and Prasad [16] have demonstrated the phenomenon of amplitude death for hidden attractors in coupled oscillator systems. More recently, considering a model of a power electronic relay system with hysteresis, Zhusubaliyev *et al* [17] have described a variety of different bifurcations through which hidden attractors can arise in a realistic technical control system.

These findings obviously lead to questions about the origin of the quasiperiodic and chaotic states observed in systems that do not display an unstable equilibrium point. However, besides such important conceptual issues, the absence of an unstable equilibrium state also leads to a number of interesting problems relating to the localization of the complex states in phase space [18, 19]. It is well-known that nonlinear dynamic systems with two or more coexisting stable states can display basins of attraction with complicated (i.e., fractal) boundaries [20, 21]. These situations are characterized by a position of the corresponding unstable states on the boundary between the basins of attraction for the involved stable states. In numerical studies, this form of complexity may lead to difficulties in the location of the attracting states, and specialized numerical techniques may be required to avoid missing out on some of these states [20, 21]. Similar difficulties may arise in practice when trying to direct a multistable technical control system into a particular mode of operation [22, 23]. Even for simple mechanical systems with a few coexisting stable equilibrium points, the basins of attraction can become mixed to such a degree that it is impossible in practise to initiate the trajectory of the system with the aim of reaching a specific outcome [24].

In cases where the basin of attraction for the stable state overlaps with the neighborhood of an unstable equilibrium point the situation is quite simple [18, 19]. In such cases, one can choose an initial condition close to the equilibrium point (but away from its stable manifold) and follow the transient behavior of the system until it asymptotically approaches the searched state. This option is not available if there is no unstable equilibrium point and, by analogy with the term 'hidden oscillations' introduced in connection with the classic discussion of Hilbert–Kolmogorov type problems [19], the numerical difficulties associated with the location of complex nonlinear states whose basin of attraction does not overlap with the neighborhood of an unstable equilibrium point has led to introduction of the term 'hidden

attractor' for stable (quasiperiodic or chaotic) states whose basin of attraction does not overlap with an unstable equilibrium point [18, 19].

The purpose of the present paper is to examine the formation and restructuring of hidden periodic, quasiperiodic, and chaotic attractors in an autonomous, smooth, 3D model of a radio-physical oscillator system. We first discuss the mechanisms responsible for maintaining the oscillatory dynamics in the radio-physical system and provide an overview of the mode distribution in 2D parameter space. By scanning this distribution for parameter values where the system displays quasiperiodic dynamics intervened by resonance intervals with period-doubling cascades and transitions to chaos, we follow a couple of characteristic bifurcation sequences and demonstrate the coexistence of several pairs of hidden attractors.

2. Description of the radio-physical oscillator system

Let us consider the three-dimensional autonomous oscillator system

$$\frac{\mathrm{d}^2x}{\mathrm{d}t^2} = \left(\lambda + z + x^2 - \beta x^4\right)\frac{\mathrm{d}x}{\mathrm{d}t} - \omega_0^2 x, \tag{1a}$$

$$\frac{\mathrm{d}z}{\mathrm{d}t} = \mu - x^2 \tag{1b}$$

recently proposed by Kuznetsov *et al* [12, 13] as an example of a minimum system that can display quasiperiodic behavior. These equations may be thought of as describing a generator of hard oscillations (1*a*) coupled to a rechargeable power source (1*b*). At the same time, these equations are related to formulations that have been used to demonstrate the existence of structurally stable chaos in continuous-time systems [25, 26]. In connection with the present discussion, we first note that for values of μ different from zero, the system defined by equations (1*a*) and (1*b*) does not allow for the existence of any equilibrium point, neither stable nor unstable. Only if the maximum charging rate $\mu = 0$ will the system display an equilibrium point. It is interesting to note, however, that this equilibrium point exhibits a pair of purely imaginary eigenvalues. Hence, the system will be non-hyperbolic for $\mu = 0$, or, in other words, the equilibrium point undergoes a Hopf bifurcation in its only point of existence. This situation appears to be generic of many of the systems that are known to display hidden chaotic attractors [14].

The subcritical nature of the Hopf bifurcation produced by the generator element defines the thresholds for different types of behavior in the system and also introduces a form of hysteresis. The generator frequency and the degree of sub-criticality are controlled by the parameters ω_0 and β, respectively. The term proportional to z in equation (1*a*) introduces a modulation of the rate of growth of the generator oscillations that depends on the charging state z of the storage element. Equation (1*b*) describes the storage element as a power source that is continuously charged at a rate μ and discharged at a rate proportional to the intensity x^2 of the oscillations generated by the threshold element. In the present work, the parameters λ and β will be kept constant at $\lambda = 0$ and $\beta = 0.5$.

With appropriate parameter values, the temporal behavior of the coupled system may be described in terms of the following sequence of three phases that continues to repeat itself:

(a) starting in a situation where the storage variable z is negative and close to its minimum, the generator (1*a*) operates in a regime of stable equilibrium dynamics, and existing oscillations in x gradually decrease. This allows the storage element (1*b*) to recharge at increasing speed.

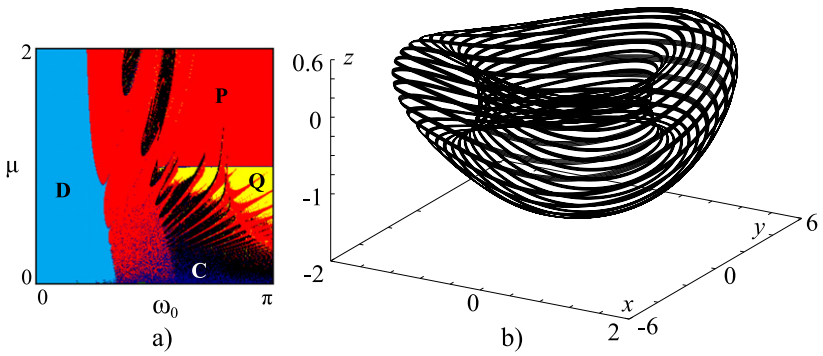

Figure 1. (a) Chart of dynamical modes in the (ω_0, μ) parameter plane. $\lambda = 0$ and $\beta = 0.5$. **D** denotes divergent dynamics, **P** denotes periodic dynamics, and **Q** and **C** denote quasiperiodic and chaotic dynamics, respectively. (b) 3D phase portrait of the quasiperiodic attractor that exists in the coupled oscillator system (1*a*) for $\mu = 0.9$ and $\omega_0 = \pi$. In this figure, the variable y represents the first derivative of x.

(b) As z becomes positive, the generator element undergoes a subcritical Hopf bifurcation and, seeded by remaining small amplitude oscillations of x, the amplitude of these oscillations begins to increase rapidly. This leads to a faster discharging of the storage element, and z again begins to decrease.
(c) Due to the subcritical nature of the Hopf bifurcation, the amplitude of the generator oscillations remains large, until z becomes sufficiently negative. The generator oscillations then again start to decrease in amplitude, leading to decreasing discharging rates for the storage element, etc.

Figure 1(a) shows the distribution of dynamical modes for the coupled oscillator system in the (ω_0, μ)-plane. As previously noted, ω_0 represents the basic oscillator frequency for the generator, and μ determines the maximum charging rate for the storage element. The remaining parameters $\lambda = 0$ and $\beta = 0.5$. The red region denoted **P** represents parameter sets that produce periodic solutions. The yellow region **Q** represents quasiperiodic dynamics, and the regions **C** (black) and **D** (blue) represent, respectively, chaotic and divergent behavior. Note, however, that several regions display coexisting attracting states of different types.

At the transition between periodic and divergent dynamics, the oscillatory mode disappears as its amplitude explodes. The chaotic (black) regions in the upper left side of the diagram represent cascades of period-doubling bifurcations associated with the period-1 and period-2 cycles, respectively. The horizontal line between the periodic and quasiperiodic regimes at $\mu = 1$ represents a secondary Hopf (or torus-birth) bifurcation that involves a new oscillatory mode into the dynamics. Finally, the (red) swallow-tail structures [27] in the quasiperiodic regime are regions of periodic resonance dynamics. This explains how the complex nonlinear dynamic phenomena, i.e. the hidden chaotic and quasiperiodic attractors, develop from the divergent dynamics that exists to the left in the figure. As an example, figure 1(b) shows a phase portrait of the quasiperiodic attractor that exists for $\mu = 0.9$ and $\omega_0 = \pi$.

3. Bifurcation structure and coexisting attractors

Considering the dense set of resonance tongues that exists in the quasiperiodic regime, a scan through this regime is likely to demonstrate a significant number of transitions between

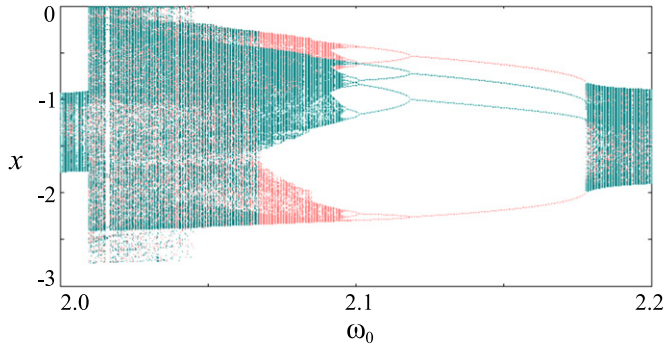

Figure 2. Bifurcation diagrams obtained by scanning the interval around the 2:1 resonance region with initial conditions that produce clockwise (red), respectively anti-clockwise (blue) rotations in the generator (x, $\dot{x}$) dynamics. At both ends, the bifurcation diagram displays coinciding (clockwise and anti-clockwise) quasiperiodic dynamics. A pair of mutually symmetric period-2 cycles are born in a saddle-node bifurcation at $\omega_0 \simeq 2.178$. As the basic frequency of the oscillator is reduced, the period-2 cycles undergo simultaneous period-doubling bifurcations accumulating in the transition to chaos for $\omega_0 \simeq 2.095$. $\mu = 0.9$.

different hidden attractors. Closer examination of the equations of motion reveals that both equations (1*a*) and (1*b*) remain invariant under the replacement of x by $-x$. This implies that the solutions to our system come either in the form of individual trajectories that are invariant to the direction of rotation for the x-oscillator, or they come as pairs of mutually symmetric solutions that rotate clock- and anti-clockwise, respectively. Phase space projections can be used to distinguish between mutually symmetric resonance cycles, and the same approach can be used to distinguish coexisting chaotic attractors as long as they have not started to intersect. When such intersection occurs, the chaotic solutions melt together to form a single symmetric solution. This occurs in a so-called attractor mergence crisis [21, 28]. A similar approach cannot be used to distinguish the mutually symmetric quasiperiodic attractors since the clock- and anti-clockwise quasiperiodic solutions live on the same geometrical structure. Let us finally note that whereas resonance cycles belonging to even resonances tend to appear in symmetric pairs, resonance cycles belonging to odd resonances tend to be born as single, symmetric solutions. Such solutions must undergo a symmetry breaking pitchfork bifurcation before period doubling can occur [20].

Figure 2 illustrates some of these points. Here we have superimposed a pair of one-dimensional bifurcation diagrams obtained by scanning the interval $2.0 < \omega_0 < 2.2$ for $\mu = 0.9$, i.e., across the region of resonant period-2 dynamics. Using $\dot{x} = 0$ as a Poincaré plane, the two scans were initiated with conditions (x_i, $\dot{x}_i = 0$, z_i) or ($-x_i$, $\dot{x}_i = 0$, z_i) to produce either clockwise or anti-clockwise rotation for the generator dynamics (x, $\dot{x}$). The scans were performed from right to left with so-called adiabatic initial conditions i.e., for each new value of ω_0 the initial conditions were chosen as the final state (x_f, $\dot{x}_f = 0$, z_f) attained for the previous value of ω_0. Red and blue diagrams represent different directions of rotation. In the parameter region where the two chaotic attractors mix, the direction of rotation is clearly not conserved. In the region of quasiperiodic dynamics, the clockwise and anti-clockwise motions take place on the same geometrical structure.

To the right in the bifurcation diagram we observe the coinciding quasiperiodic attractors that exist outside the resonance zones. As we move towards lower values of ω_0, the resonance

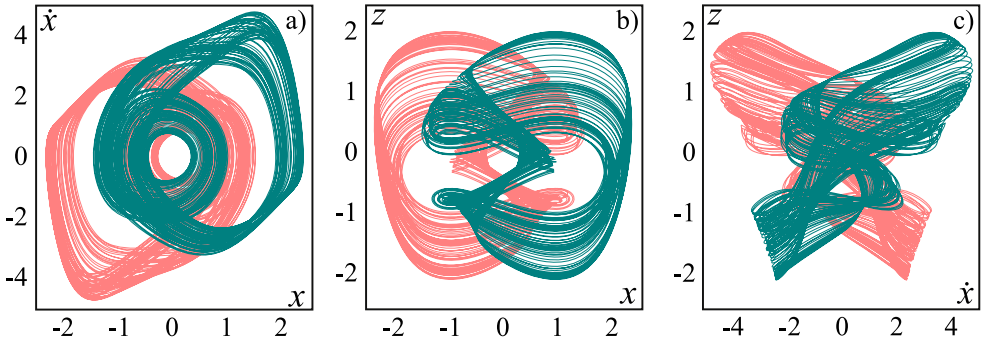

Figure 3. Three different projections of the mutually symmetric chaotic attractors that exist for $\mu = 0.9$ and $\omega_0 = 2.075$. Because of the symmetry of the equations of motion, the hidden chaotic attractors are born in pairs of mutually symmetric solutions.

domain starts at $\omega_0 \simeq 2.178$ with the appearance of two symmetric 2:1 resonance solutions (drawn in blue and red, respectively). At $\omega_0 \simeq 2.118$, simultaneous period-doubling cascades are initiated for the two period-2 solutions, and these cascades accumulate with the transition to chaos for $\omega_0 \simeq 2.095$. With further reduction of ω_0, the chaotic attractors continue to grow until they finally intersect and mix in an attractor mergence crisis at $\omega_0 \simeq 2.063$. Hereafter the system only displays a single chaotic state and, after another (presumably interior) crises at $\omega_0 \simeq 2.044$, the chaotic attractor finally collapses in a boundary crisis at which both the attractor and its basin of attraction disappear. This happens at $\omega_0 \simeq 2.010$, and the system hereafter returns to the quasiperiodic solutions that exist outside the resonance domain.

The term crises [28] denotes sudden changes in the size or form of a chaotic attractor associated, for instance, with the collision with another chaotic attractor or with an unstable periodic cycle. In an attractor mergence crisis two chaotic attractors intersect and merge into a single, larger chaotic attractor. In an interior crisis the chaotic attractor collides with an unstable cycle, typically stemming from an 'earlier' step of the bifurcation cascade. This may lead to either an abrupt increase or an abrupt decrease of the size of the attractor. Finally, in a boundary crisis, the chaotic attractor collides with its basin boundary and both the attractor and its basin of attraction disappear. Note, however, that the above distinction between different types of crises is based on the observed characteristic variations of the stable chaotic attractors combined with experience from other systems. Precise distinction requires methods (such as continuation) that would allow us to also follow the unstable orbits.

Figures 3 (a, b and c) show 2D phase projections of the coexisting hidden chaotic attractors that exist in the coupled oscillator system for $\mu = 0.9$ and $\omega_0 = 2.075$. It is easy to appreciate the mutual symmetry of the two attractors that can be reached from different initial states. Figure 4(a) provides a 3D phase portrait of the same attractors, and figure 4(b) shows a Poincaré section for the chaotic attractors with the Poincaré plane $\dot{x} = 0$. This figure illustrates in particular the two-band structure of the individual chaotic attractors. Finally, figures 5(a) and (b) show 2D projections of the phase portraits for the merged chaotic attractors that exist for $\omega_0 = 2.05$ and 2.019, respectively. It is interesting to note how the merged chaotic attractor in figure 5(b) has grown in size relative to the attractor in figure 5(a) and now comes very close to the point $(x, \dot{x}) = (0, 0)$ in the projection plane.

Figure 6 shows the one-dimensional bifurcation diagram for slightly higher generator frequencies where 5:2 resonance dynamics is observed to coexist with (non-resonant) quasiperiodic dynamics. Construction of this figure has again involved a number of adiabatic

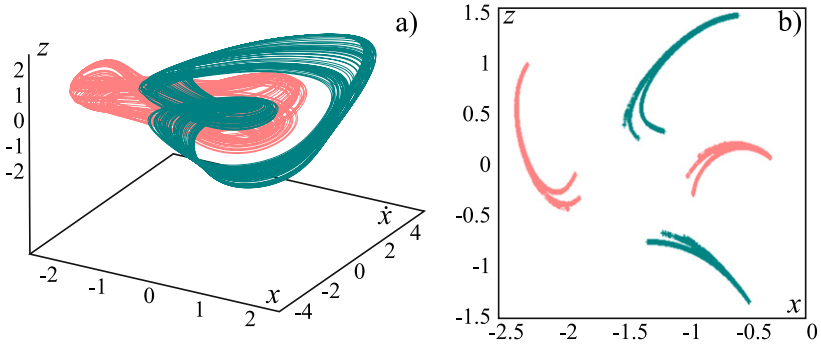

Figure 4. (a) 3D phase portrait of the coexisting hidden chaotic attractors that exist for $\mu = 0.9$ and $\omega_0 = 2.075$. (b) Poincaré sections for $\dot{x} = 0$ of the two mutually symmetric two-band attractors in (a). The two attractors can be reached with different initial conditions.

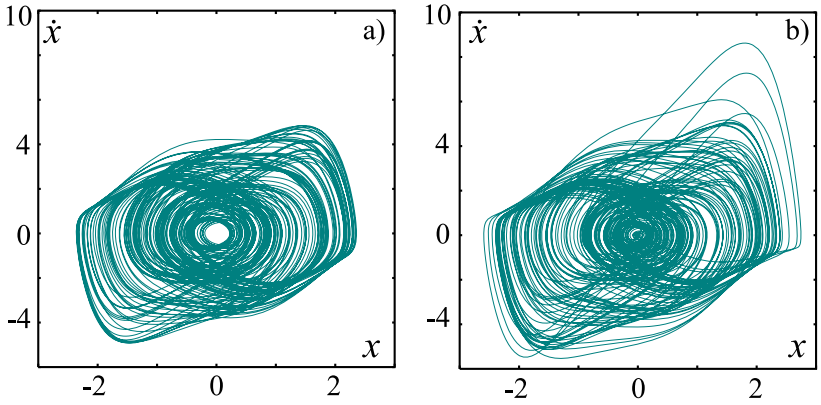

Figure 5. 2D projections of the phase portraits of system (1*a*) for $\mu = 0.9$. (a) $\omega_0 = 2.05$ and (b) $\omega_0 = 2.019$. The figure illustrates the form of the chaotic attractors after the original, mutually symmetric attractors have merged. Note how the merged chaotic attractor in (b) has expanded relative to the attractor in (a). To a large extent, this expansion is related to the crises that occurs at $\omega_0 = 2.044$.

scans with different initial conditions and different scanning directions. Note, however, that the color code differs from that of figure 2. In figure 6, red denotes the clockwise or anti-clockwise oscillatory behaviors associated with the quasiperiodic attractors. Blue and purple represent different forms of resonance dynamics [20].

The 5:2 resonance cycle is born in a saddle-node bifurcation a little to the right of the frequency interval considered in figure 6. Depending on the initial conditions this cycle may be traversed in the clockwise or in the anti-clockwise direction. Moreover, because of the symmetry, period-doubling bifurcations cannot take place until the cycle has undergone a symmetry breaking pitchfork bifurcation [20]. This occurs at $\omega_0 \simeq 2.415$, and the two mutually symmetric oscillatory modes hereafter individually proceed to chaos. At $\omega_0 = 2.381$, the mutually symmetric chaotic attractors intersect and mix in an attractor mergence crisis [21, 28], and at $\omega_0 \simeq 2.358$ the merged attractor undergoes a boundary crisis at which both the attractor itself and its basin of attraction disappear. To the left of this point,

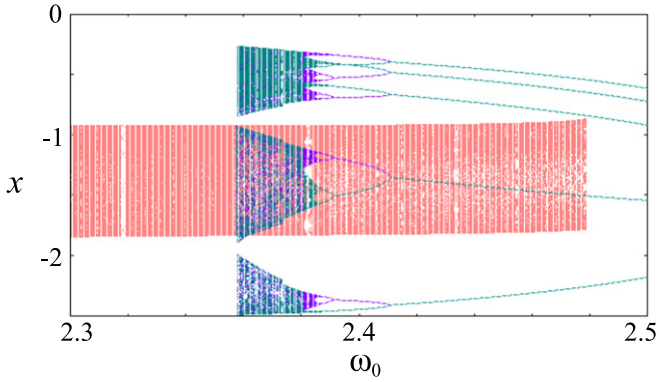

Figure 6. Bifurcation diagram obtained by superimposing scans of the interval $2.3 < \omega_0 < 2.5$ in both directions and with different initial conditions. To the right in the figure the diagram shows the symmetric period-5 resonance cycle. At $\omega_0 \simeq 2.415$, this cycle undergoes a pitchfork bifurcation followed, for decreasing values of ω_0, by a period-doubling cascades and the transition to chaos. Red elements of the diagram represent the clockwise and anti-clockwise dynamics associated with the coinciding quasiperiodic states. Blue and purple parts represent periodic, chaotic and merged chaotic states associated with the resonance dynamics.

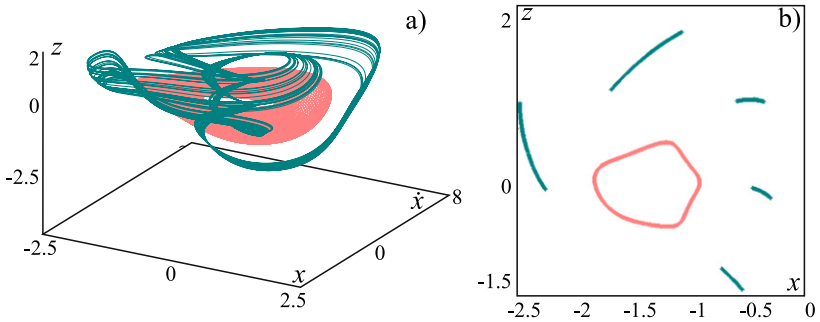

Figure 7. (a) 3D projection of phase portrait showing a quasiperiodic attractor coexisting with one of the five-band chaotic attractors that exist for $\mu = 0.9$ and $\omega_0 = 2.375$. (b) Poincaré section at $\dot{x} = 0$ for the two coexisting attractors in (a).

the considered ω_0-range only displays quasiperiodic dynamics with higher order resonance regions. In the right hand side of the bifurcation diagram, at $\omega_0 \simeq 2.478$, the quasiperiodic oscillations terminate in a homoclinic bifurcation involving the saddle cycle associated with the saddle-node bifurcation in which the original 5:2 resonance cycle was born.

Together with the quasiperiodic attractor, figure 7(a) presents a phase portrait of one of the coexisting five-band chaotic attractors born in the above described transitions. Note how the x-oscillator performs five rotations for each two rotations of the z-oscillator. Figure 7(b) shows a Poincaré section of the same two attracting states constructed from the points of intersection with the plane $\dot{x} = 0$ for $\omega_0 = 2.375$. Figure 8 (a, b and c) show a set of 2D phase space projections of the quasiperiodic attractor and the co-existing mutually symmetric five-band chaotic attractors for $\omega_0 = 2.383$, i.e., immediately to the right of the above mentioned attractor mergence crises.

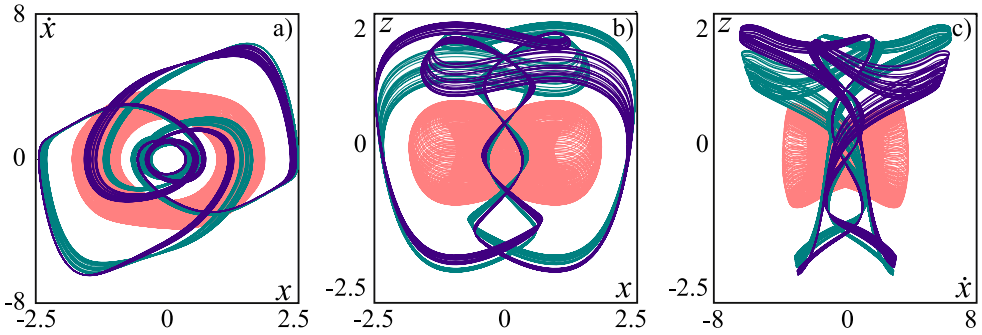

Figure 8. 2D projection of phase portraits of three co-existing hidden attractors, one quasiperiodic attractor (red) and two five-band chaotic attractors (blue and violet). $\mu = 0.9$ and $\omega_0 = 2.383$.

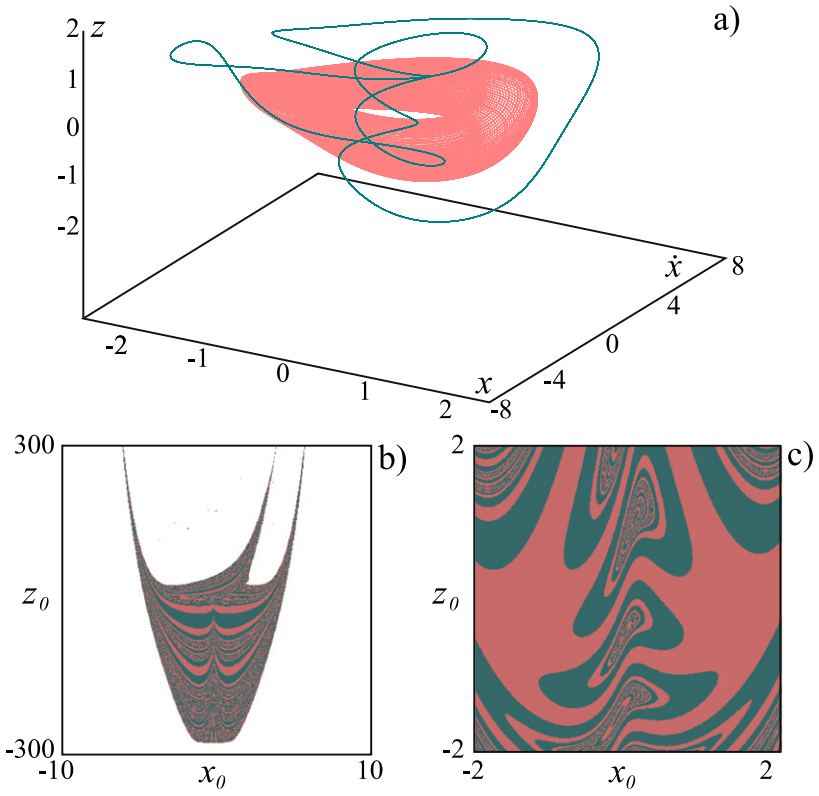

Figure 9. (a) 3D phase portraits of the attracting torus state and of one of the period-5 resonance cycles that can be observed for $\mu = 0.9$ and $\omega_0 = 2.4$. (b) Basin of attraction for the symmetric period-5 cycles (blue) and for the quasiperiodic attractor (red). (c) Magnification of part of (b). The basins of attraction were calculated for trajectories starting in the Poincaré plane $\dot{x} = 0$.

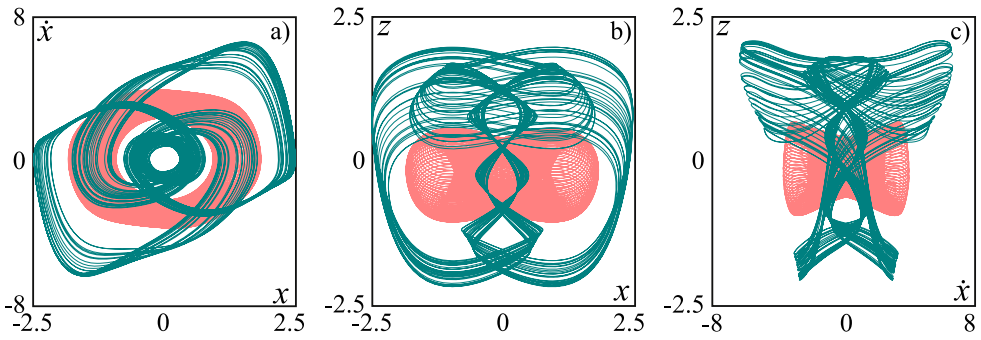

Figure 10. 2D projection of phase portraits of three co-existing hidden attractors, one quasiperiodic attractor (red) and one merged chaotic attractor (blue). $\mu = 0.9$ and $\omega_0 = 2.370$.

Figure 9(a) shows a 3D phase portrait of one of the period-5 resonance cycles that exists together with the quasiperiodic attractor for $\omega_0 = 2.37$. Figure 9(b) shows the basins of attraction for the resonant (period-5) and non-resonant (quasiperiodic) solutions as obtained for trajectories starting from the Poincaré plane $\dot{x} = 0$ with initial conditions in the intervals $-10 < x_0 < 10$, $-300 < z_0 < 300$, and figure 9(c) shows a magnification of part of figure 9(b). Initial states marked in blue approach one of the mutually symmetric period-5 cycles, and initial states marked in red approach the attracting quasiperiodic set.

Finally, figure 10 shows a set of 2D phase space projections for $\omega_0 = 2.370$, i.e. in the regime where the quasiperiodic attractors coexist with a single chaotic attractor that has developed from the merging of the two symmetric chaotic attractors in figure 8.

4. Conclusion

The concept of a 'hidden attractor' was introduced in the mid 20th century in connection with discussions among leading scientists of the field about problems associated with 'polynomial systems', 'embedded oscillations', 'stability in the large', etc [19]. If the basin of attraction for an oscillatory state overlapped with an unstable equilibrium point, the problem of locating the oscillation was relatively simple. However, with the analytic and computational techniques available at that time, the location of a limit cycle whose basin of attraction did not overlap with an unstable equilibrium point required application of very specific and cumbersome methods.

The present interest in hidden attractors derives from the observation of chaotic dynamics in autonomous systems that do not display any equilibrium point or only display stable equilibria [6, 24] . By analogy with its historical use, the term 'hidden attractor' thus refers to the existence of chaotic states whose basin of attraction does not overlap with an unstable equilibrium point. This situation no longer represents a major challenge to our numerical techniques. However, the birth of a chaotic attractor in an autonomous system with no equilibrium points still represents a challenge to our general understanding of the development of chaos. This so much more as, until a couple of years ago, chaotic systems without equilibria were commonly rejected as 'incomplete' or 'mis-formulated'. Today, more than 50 such systems are known [14, 29], and the questions of interest include (i) what are the possible mechanisms of birth for hidden chaotic attractors, (ii) do the associated bifurcation

scenarios display particular features, and (iii) do systems of this type arise in connection with concrete practical problems.

In the present paper we have demonstrated how dynamics in a model of an autonomous radio-physical oscillator system can arise in the absence of any equilibrium point. We have shown how the development to chaos takes place either via a period-doubling cascade or via a torus birth bifurcation and the subsequent formation of resonance regions in the form of a swallow tail structure. These structures also produce coexisting regions of non-resonant (quasiperiodic) and resonant (periodic and chaotic) regimes, thus providing for situations with a significant number of simultaneous complex dynamic states. We have followed the sequence of dynamic states through a couple of one-dimensional bifurcation diagrams, and we have illustrated the form of the basins of attraction.

Acknowledgments

This research was supported by the Grant of RFBR (14-02-00085) and Grant of RF President program for leading Russian research school NSh-1726.2014.2.

References

[1] Lorenz E N 1963 Deterministic nonperiodic flow *J. Atmos. Sci.* **20** 130–41
[2] Rössler O E 1976 An equation for continuous chaos *Phys. Lett.* A **57** 397–8
[3] Shil'nikov L P 1965 A case of the existence of a denumerable set of periodic motions *Sov. Math.—Dokl.* **6** 163–6
[4] Silva C P 1993 Shil'nikov's theorem—a tutorial *IEEE Trans. Circuits Syst.* I **40** 657–82
[5] Leonov G A, Kuznetsov N V, Kuznetsova O A, Seledzhi S M and Vagaitsev V I 2011 Hidden oscillations in dynamical systems *Trans. Syst. Control* **6** 54–67
[6] Leonov G A, Kuznetsov N V and Vagaitsev V I 2011 Localization of Hidden Chua's attractors *Phys. Lett.* A **375** 2230–3
[7] Leonov G A, Kuznetsov N V and Vagaitsev V I 2012 Hidden attractor in smooth Chua systems *Physica* D **241** 1482–6
[8] Wei Z 2011 Dynamical behaviors of chaotic systems with no equilibria *Phys. Lett.* A **376** 102–8
[9] Wei Z and Yang Q 2011 Dynamical analysis of a new autonomous 3D system only with stable equilibria *Nonlinear Anal.: Real World Appl.* **12** 106–18
[10] Wang Z, Cang S, Ochola E O and Sun Y 2012 A hyperchaotic system without equilibrium *Nonlinear Dyn.* **69** 531–7
[11] Wei Z, Wang R and Lin A 2014 A new finding of the existence of hidden hyperchaotic attractors with no equilibria *Math. Comput. Simul.* **100** 13–23
[12] Kuznetsov A P, Kuznetsov S P and Stankevich N V 2010 A simple autonomous quasiperiodic self-oscillator *Commun. Nonlinear Sci. Numer. Simul.* **15** 1676–81
[13] Kuznetsov A P, Kuznetsov S P, Mosekilde E and Stankevich N V 2013 Generators of quasiperiodic oscillations with three-dimensional phase space *Eur. Phys. J. Spec. Top.* **222** 2391–8
[14] Jafari S, Sprott J C and Golpayegani S M R H 2013 Elementary quadric chaotic flows with no equilibria *Phys. Lett.* A **377** 699–702
[15] Wang X and Chen G R 2013 Constructing a chaotic system with any number of equilibria *Nonlinear Dyn.* **71** 429–36
[16] Chaudhuri U and Prasad A 2014 Complicated basins and the phenomenon of amplitude death in coupled hidden attractors *Phys. Lett.* A **378** 713–8
[17] Zhusubaliyev Zh, Mosekilde E, Rubanov V G and Nabokov R A 2015 Multistability and hidden attractors in a relay system with hysteresis *Physica* D submitted
[18] Bragin V O, Vagaitsev V I, Kuznetsov N V and Leonov G A 2011 Algorithms for finding hidden oscillations in nonlinear systems. The Aizerman and Kalman conjectures and Chua's circuits *J. Comput. Sci. Int.* **50** 511–43

[19] Leonov G A and Kuznetsov N V 2013 Hidden attractors in dynamical systems: From hidden oscillation in Hilbert–Kolmogorov, Aizerman and Kalman problems to hidden chaotic attractor in Chua circuits *Int. J. Bifurcation Chaos* **23** 1330002
[20] Ueda Y 1991 Survey of regular and chaotic phenomena in the forced Duffing oscillator *Chaos Solitons Fractals* **1** 199–231
[21] Grebogi C, Ott E and Yorke J A 1987 Basin boundary metamorphoses: changes in accessible boundary orbits *Physica* D **24** 243–63
[22] Zh T, Zhusubaliyev O O and Yanochkina E 2011 Mosekilde: coexisting tori and torus bubbling in non-smooth systems *Physica* D **240** 397–405
[23] Zhusubaliyev Zh T, Mosekilde E and Pavlova E V 2013 Multistability and torus reconstruction in a DC/DC converter with multilevel control *IEEE Trans. Ind. Inform.* **9** 1937–46
[24] Feldberg R, Szymkat M, Knudsen C and Mosekilde E 1990 Iterated map approach to die tossing *Phys. Rev.* A **42** 4493–502
[25] Kuznetsov S P and Pikovsky A 2007 Autonomous coupled oscillators with hyperbolic strange attractors *Physica* D **232** 87–102
[26] Isaeva O B, Kuznetsov S P and Mosekilde E 2011 Hyperbolic chaotic attractor in amplitude dynamics of coupled self-oscillators with periodic parameter modulation *Phys. Rev.* E **84** 016228
[27] Glass L and Perez R 1982 Fine structure of phase locking *Phys. Rev. Lett.* **48** 1772–5
[28] Grebogi C, Ott E and Yorke J A 1982 Chaotic attractors in crisis *Phys. Rev. Lett.* **48** 1507–10
[29] Molaie M, Jafari S, Sprott J C and Golpayegani S M R H 2013 Simple chaotic flows with one stable equilibrium *Int. J. Bifurcation Chaos* **23** 1350188